C.I. Bajer i B. Dyniewicz. Space-time approach to numerical analysis of a string with a moving mass. Int. J. Numer. Meth. Engng., v. 78(10), 2008, pp. 1528-1543.

Space-time approach to numerical analysis of a string with a moving mass

Czesław I. Bajer and Bartłomiej Dyniewicz

Institute of Fundamental Technological Research,
Polish Academy of Sciences,
Świętokrzyska 21, 00-049 Warsaw, Poland

November 30, 2013

Abstract

Inertial loading of strings, beams and plates by mass travelling with near-critical velocity has been a long debated. Typically, a moving mass is replaced by equivalent force or an oscillator (with "rigid" spring) that is in permanent contact with the structure. Such an approach leads to iterative solutions or imposition of artificial constraints. In both cases rigid constraints result in serious computational problems. a direct mass matrix modification method frequently implemented in the finite element approach gave reasonable results only in the range of relatively low velocities. In this paper we present the space-time approach to the problem. The interaction of the moving mass/supporting structure is described in a local coordinate system of the space-time finite element domain. Resulting characteristic matrices include inertia, Coriolis and centrifugal forces. Simple modification of matrices in the discrete equations of motion allows us to gain accurate analysis of a wide range of velocities, up to the velocity of the wave speed. Numerical examples prove the simplicity and efficiency of the method. The presented approach can be easily implemented in the classic finite element algorithms.

keywords: moving mass, inertial load, space-time finite element method, space-time approach, finite element method, vibrations of string

1 Introduction

Inertial loads moving on strings, beams and plates with sub or super critical velocities are of special interest to practising engineers. Theoretical and numerical solutions are applied to problems with single or multi-point contact such as: train-track or vehicle-bridge interaction, pantograph collectors in railways, magnetic railways, guideways in robotic technology, etc.

First the difference between the inertial loading and loading by moving mass-less force must be emphasised. In the inertial load problem the moving mass is placed directly on the structure (Fig. 1*a*), while the massless force represents the equivalent influence of inertia, or is typically modelled as a spring–mass system load (Fig. 1*b*). The present paper deals

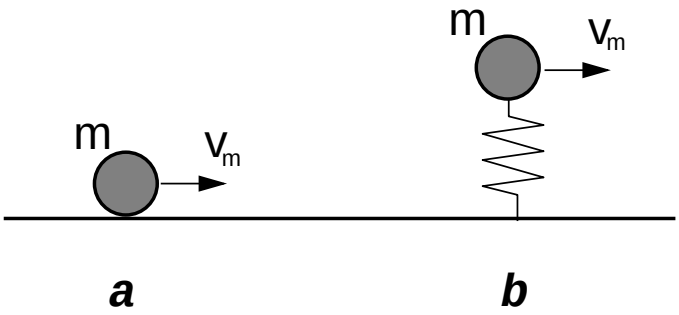

Figure 1: Moving mass (a) and moving oscillator (b).

with the first type of loading. Commonly, differential equations derived for moving mass problems are solved numerically by using finite element techniques. Yet, this approach has considerable disadvantages. As long as a mass influence is considered as an equivalent force system, computations can be performed with sufficient accuracy, but only in low range of travelling speed (up to 0.2 of the wave speed in a string). The moving object is joined to the string or beam with a spring/absorber system. Then the "equivalent" force is determined, with the assumption of relatively high stiffness of the spring. This results in some serious numerical difficulties. On the other extreme, the "soft way" contact is assumed [1]. The formulation of numerical procedures requires establishing force equilibrium in discrete time points. Governing differential equations are not consequently considered in the time intervals. Although time integration is performed by relatively accurate procedures, the physical problem is treated separately from the time integration scheme. This is the reason why strongly nonlinear problems cannot be easily solved by traditional approaches.

Analysis of the moving mass problem is widely presented in the literature. The closed solution exists in the case of mass moving on a massless string [2, 3]. Otherwise the final results are obtained numerically, although the solution is preceded by complex analytical calculations. In numerous references, authors treat the problem in a low range of the mass speed. In such a case, the results are sufficient, even if the inertial term contributing to moving mass is not correctly treated by the time integration method. Simply, the moving mass influence, in such cases, is minor compared with static displacements.

Theoretical approaches were intensively published, starting from the beginning of the twentieth century (for example [4, 5, 6]). Smith [7] proposed the purely analytical solution for the inertial moving load, however, in the case of the massless string only. Broad analysis of moving loads was given in [3, 8]. In recent contributions complex problems of structures subjected to the moving inertial load [9] or oscillator [10, 11, 12] were analysed. Variable speed of the load was considered for example in [13, 14, 15]. Unfortunately, the beam was subjected there to the massless forces. The equivalent dynamic mass influence is analysed in [16]. The infinitely long string subjected to a uniformly accelerated point mass was also treated [17] and analytical solution of the problem concerning the motion of an infinite string on Winkler foundation subjected to an inertial load moving at a constant speed was given [18].

Measurements of the wave speed in railway tracks treated as beams show values 800–1000 km/h. In the case of soaked ground the speed can decrease to 500 km/h or less. Dynamic influence of the moving load significantly increases the structure deflection. The highest dynamic contribution determines the critical speed of motion. Practically, the critical mass speed equals to 0.4–0.5 of the wave speed. This is the range of modern vehicle motion.

Numerical approaches implemented in the commercial codes are acceptable only for low speed. Moreover, the moving mass is usually introduced as a set of oscillators, joined elastically or viscoelastically to the main structure. Rigidity of the artificial string cannot be high enough due to the computational limitations. This coupled non-linear problem must be solved iteratively or by imposition of complex constraint. The dynamic problem can be solved in one iteration per time step, however, with the loss of accuracy, and what is essential, only in the low speed range.

The dynamic problem can be considered as a sequence of static solutions, performed step-by-step with a prescribed time increment. At a low velocity of the mass (approximately up to 0.1 of the critical speed and up to 0.2 of the wave speed in the unloaded and unballasted structure) simple replacement of the mass from joint to joint, or from element to element, can be applied with an error sufficiently low for engineering purposes. However, the error dramatically increases with the travelling speed, and such an approach cannot be applied in a general case. Direct modification of global characteristic matrices in the discrete system is attractive since it allows us to avoid computational complexity as in the case of moving oscillators or the imposition of supplementary constraints.

The paper [19] presents an early research in the field of discrete solutions of moving mass problems. The beam was subjected to a moving concentrated mass together with an oscillator. The moving mass was placed directly on the beam contributed load terms obtained by the chain rule derivation, called also the Renaudot formula. The problem was solved typically in two stages. The beam forced kinematically on the oscillator motion, and then the oscillator acted with a force to the beam. While zeroing the oscillator mass one should obtain solutions for pure mass motion. The presented results cannot be simply compared with analytical solutions in higher speed range.

In the next paper [20], the moving oscillator is being considered. The solution with spring stiffness tending to infinity should approach the solution with moving mass. Unfortunately, final numerical tests exhibit significant errors for higher spring stiffness. In [21] the moving inertial load is distributed on a given segment. The approach is similar to the Filho solution [19], in the case of zero oscillator mass. Increasing mass velocity decreases the accuracy of the results. Another approach is presented in [9], where a declined beam element is considered. The author proves that the influence of the Coriolis force is minor, when compared with total beam response. The numerical solution obtained with the above method for the string vibration problem is divergent (Fig. 2). In the case of a beam the divergence rate is lower then for a string, because of type of the differential equation.

Here, we must notice the difference in equations that describe beam and string motion. In the case of beam motion, both of the Euler and Timoshenko type, we have a significant influence of bending. The equation is a hyperbolic–parabolic type. In the case of string motion, we have a hyperbolic equation with a pure wave propagation. This determines the different features of the numerical solution of both problems. This is probably the reason why numerical solutions of the problem of moving mass travelling on the string are rarely presented in publications.

In this paper, we intend to discuss numerical aspects of moving mass, placed directly on the structure. The influence of moving force alone is trivial, and this question will not be discussed. The moving mass cannot be simply incorporated in the discrete formulation. The space-time formulation [22, 23, 24, 25, 26, 27] is used to derive matrices which contribute to the moving mass effect. Consequent formulation results in a proper time stepping scheme. The space-time finite element formulation seems to be the best approach to formulate the problem, and to derive respective characteristic matrices of the step-by-step procedure of

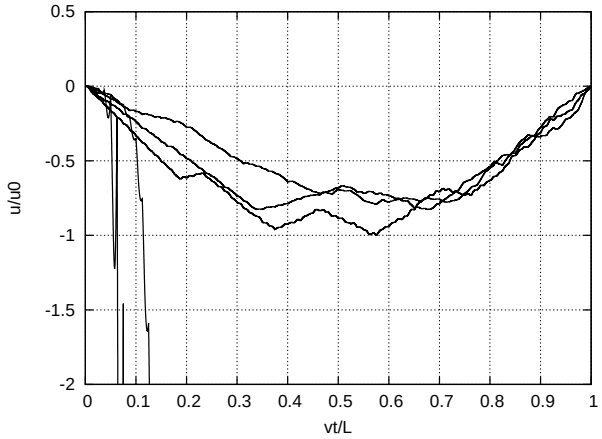

Figure 2: Divergence of the numerical solution, based on [19], for the ratio $m/\rho AL = 0.1$.

time integration of the nonlinear motion equation. The analytical-numerical solution of the problem exhibits discontinuity of the particle trajectory at the end support. This phenomenon is visible in discrete solutions aswell. It results in an increasing solution error in higher speed of the moving mass at the final stage of the motion.

The method can be considered as the extension of the traditional finite elements method in the time domain. The first attempts at the space-time modelling of physical problems were published in [28]. The definition of the minimized functional allowed the relationship between time and spatial variables to derive in space–time subdomains. These subdomains can be considered as space-time finite elements. Oden [29] proposed a general approach to the finite element method. He extended the image of the structure in the time variable. Unfortunately, this idea of non-stationary partition of structure on subspaces was not continued. We can also recall some other publications [30, 31, 32, 33] as a historical background. Kaczkowski introduced for the first time some abstract physical terms to mechanics: the equation of time-work, mass as a vector quantity or a space-time rigidity [34, 35, 36]. Triangular elements of string were elaborated. Then non-stationary partition of the structure and non rectangular space-time elements [22, 23] enabled the solution of a new group of problems by the space-time element method: problems with adaptive mesh [1, 24, 25], contact problems [37, 38], and large deformations [39].

2 Formulation of the problem

Let us consider a string of the length l, cross-sectional area A, mass density ρ, tensile force N, subjected to a concentrated mass m accompanied by a point force P (Fig. 3), moving with a constant speed v_m. The motion equation of the string under the moving inertial load with a constant speed v_m has a form

$$-N\,\frac{\partial^2 u(x,t)}{\partial x^2} + \rho A\,\frac{\partial^2 u(x,t)}{\partial t^2} = \delta(x-v_m t)\,P - \delta(x-v_m t)\,m\,\frac{\partial^2 u(v_m t,t)}{\partial t^2}\,. \quad (1)$$

We impose boundary conditions $u(0,t) = 0,\ u(l,t) = 0$ and initial conditions $u(x,0) = 0,\ \partial u(x,t)/\partial t\,|_{t=0} = 0$.

The problem can easily be solved analytically or numerically if P is the only travelling factor. Respective closed solutions or solutions in a form of series expansion exist in such

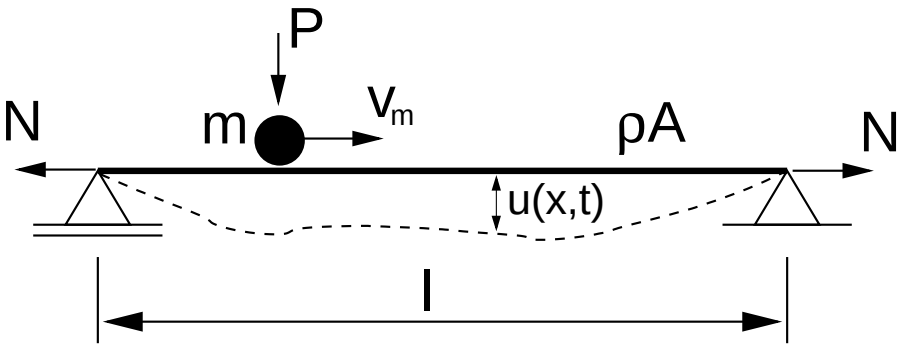

Figure 3: Moving inertial load.

a case. However, in our paper we concentrate on the influence of the inertial moving term. We only consider small displacements of the string.

3 Theoretical analysis

The general semi-analytical solution is given below for two reasons. First, we use it as a reference solution to be compared with the numerical results. Secondly, we intend to emphasize discontinuity of the mass trajectory at the end support. This important property is visible both in semi-analytical, and numerical results and influences the response of more complex systems. The final solution is obtained as a matrix differential equation of the second order. Numerical integration results in the solution in a full range of the velocity. We can mention here that exactly the same approach can be applied to a beam with a moving mass.

3.1 Semi-analytical solution

We present here an analytical approach, discussed in the extended form in [40]. It will be a base for comparison of numerical results given in the following sections.

In order to reduce the partial differential equation to an ordinary differential equation, we apply the Fourier sine integral transformation in a finite range $< 0, l >$

$$V(j,t) \;=\; \int_0^l u(x,t)\,\sin\frac{j\pi x}{l}\,\mathrm{d}x \quad u(x,t) \;=\; \frac{2}{l}\,\sum_{j=1}^{\infty} V(j,t)\,\sin\frac{j\pi x}{l} \quad . \tag{2}$$

The motion equation after the Fourier transformation is presented as:

$$\begin{aligned} \ddot{V}(j,t) \;+\; \alpha\sum_{k=1}^{\infty}\ddot{V}(k,t)\,\sin\omega_k t\,\sin\omega_j t \;+\; 2\alpha\sum_{k=1}^{\infty}\omega_k\,\dot{V}(k,t)\,\cos\omega_k t\,\sin\omega_j t \;+ \\ +\; \Omega^2\,V(j,t) \;-\; \alpha\sum_{k=1}^{\infty}\omega_k^2\,V(k,t)\,\sin\omega_k t\,\sin\omega_j t \;=\; \frac{P}{\rho A}\,\sin\omega_j t \;, \end{aligned} \tag{3}$$

where

$$\omega_k \;=\; \frac{k\pi v_m}{l}\;, \qquad \omega_j \;=\; \frac{j\pi v_m}{l}\;, \qquad \Omega^2 \;=\; \frac{N}{\rho A}\,\frac{j^2\pi^2}{l^2}\;, \qquad \alpha \;=\; \frac{2m}{\rho A\,l}\;. \tag{4}$$

The analytical solution to this problem does not exist. We must solve this equation numerically. The equation (3) is written in a matrix form, where matrices **M**, **C** and **K** are square matrices $(j, k = 1...n)$

$$\mathbf{M}\ddot{\mathbf{V}} + \mathbf{C}\dot{\mathbf{V}} + \mathbf{K}\mathbf{V} = \mathbf{P} \ , \tag{5}$$

where the matrices elements are as follows:

$$m_{ij} = \alpha \sin\frac{i\pi v_m t}{l} \sin\frac{j\pi v_m t}{l} + \delta_{ij} \ , \tag{6}$$

$$c_{ij} = 2\alpha \frac{j\pi v_m t}{l} \sin\frac{i\pi v_m t}{l} \cos\frac{j\pi v_m t}{l} \ , \tag{7}$$

$$k_{ij} = \frac{i^2\pi^2}{l^2}\frac{N}{\rho A}\delta_{ij} - \alpha\frac{j^2\pi^2 v_m^2}{l^2} \sin\frac{i\pi v_m t}{l} \sin\frac{j\pi v_m t}{l} \ , \tag{8}$$

and the vector elements:

$$p_i = \frac{P}{\rho A} \sin\frac{i\pi v_m t}{l} \ , \tag{9}$$

$$v_i = V(i,t) \ . \tag{10}$$

δ_{ij} is the Kronecker delta. When coefficients $V(j,t)$ are computed, displacements of the string (2) constitute the solution of (1). It is the solution for a full range. We can calculate displacement in each point of string and for all values of v_m.

3.2 Results of semi-analytical calculations

The integration of the equation (5) results in components which describe displacements in time (2). Thus the time-space plot of the deflected string can be done (Fig. 4). Four velocities v_m=0.3, 0.5, 1.0, 1.2 were selected. For our purpose we depict the mass trajectory as a section of this 3-dimensional domain. Fig. 5 presents results for the same set of velocities.

The analysis of results exhibits a jump of the mass in the neighbourhood of the end support. In the paper [40] the discontinuity of the mass trajectory near the end support was mathematically proven. The proof can be given in the case of massless string. This solution enabled us to prove the jump of the trajectory in the whole range of the speed $0 < v_m \leq c$. This conclusion has minor practical meaning since we consider the small displacement case for which $(\partial u/\partial t)^2 << 1$. Yet, it is important for further numerical investigations and conclusions. What is more, this exhibited property results in significant inconveniences in discrete solutions.

In the case of inertial string the pure mathematical proof cannot be given. Numerical integration of the second order differential equation (5) results in a similar feature. One can notice significant discontinuity range. Space-time plots demonstrate wave fronts and reflections both from supports and the moving mass. Especially for v_m=0.5c the moving mass approaches the end support in a phase of deep vertical displacement. In spite of low convergence of the sum (2) good accuracy of results was obtained. We can notice the sharp edge of the wave and reflection from both supports. Moreover, the wave reflection from the travelling mass is easily visible, especially for the case $v_m = 1.2c$. Both the mass trajectory, and waves are depicted.

A global analytical solution can be considered as a reference solution. It is relatively simple. Although it is valid for the whole range of the speed v_m (sub-critical, critical and over-critical), it can be used only in a limited range of practical problems.

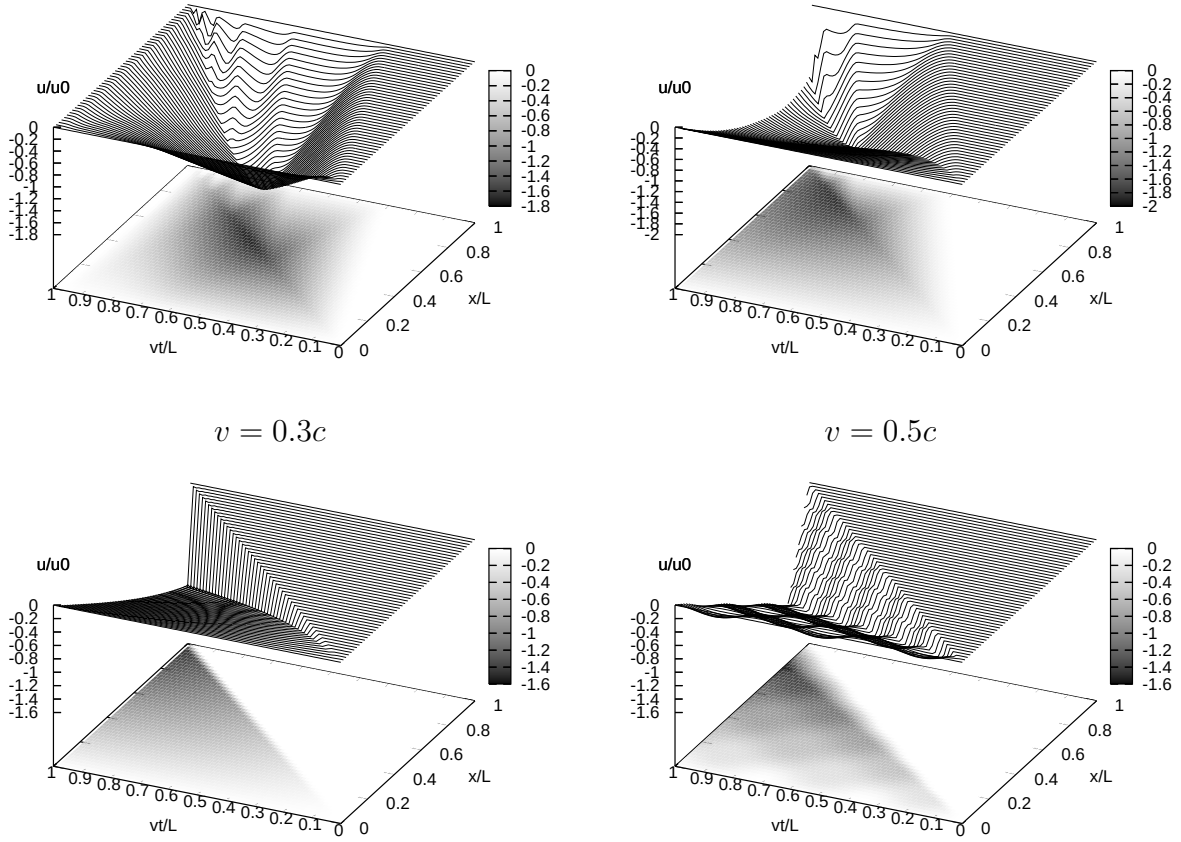

$v = 0.3c$ $v = 0.5c$

$v = 1.0c$ $v = 1.2c$

Figure 4: Simulation of the string motion under the mass moving at v_m=0.3c, 0.5c, 1.0c and 1.2c.

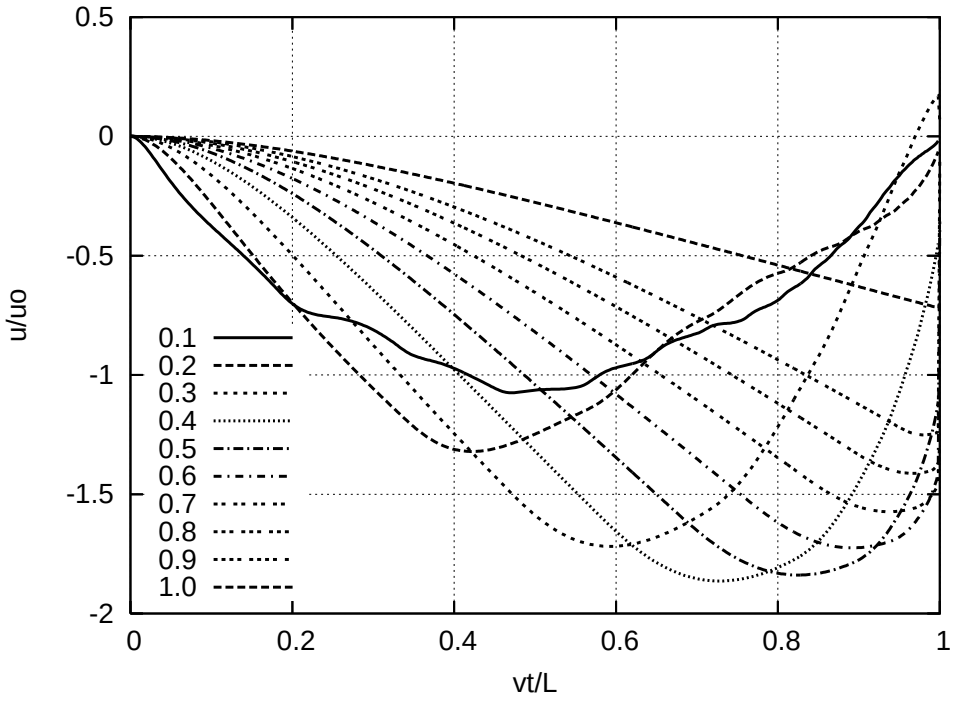

Figure 5: Displacements computed semi-analytically with Eqn. (5) at various speeds.

4 Space-time finite element approach

The numerical analysis of the problem of the moving inertial load can be performed with the use of the space-time finite element method.

4.1 Discretization of the string

We consider Eqn. (1) in the space-time domain $\Omega = \{(x,t)\colon 0 \le x \le b, \quad 0 \le t \le h\}$. The equation of the virtual power is obtained by multiplying (1) by the virtual velocity $v^*(x,t)$. The total virtual power in Ω is equal to

$$\int_0^h \int_0^b v^*(x,t) \left(\rho A \frac{\partial^2 u}{\partial t^2} - N \frac{\partial^2 u}{\partial x^2} - \eta \frac{\partial u}{\partial t} \right) \mathrm{d}x \, \mathrm{d}t = 0 \ . \tag{11}$$

η denotes internal damping coefficient. Integrating (11) by parts with respect to x results in

$$\rho A \iint_\Omega v^* \frac{\partial v}{\partial t} \, \mathrm{d}\Omega + N \iint_\Omega \frac{\partial v^*}{\partial x} \frac{\partial u}{\partial x} \, \mathrm{d}\Omega + \iint_\Omega \frac{\partial v^*}{\partial x} \varepsilon_0 \, \mathrm{d}\Omega - \eta \iint_\Omega v^* v \, \mathrm{d}\Omega = 0 \ . \tag{12}$$

We assume linear variation of velocity $v = \partial u / \partial t$ with x and t:

$$v(x,t) = \sum_{i=1}^{4} N_i(x,t) \, v_i \ . \tag{13}$$

In the domain Ω the shape function $\mathbf{N} = [N_1, \ldots, N_4]$ has a form:

$$\mathbf{N} = \left[\frac{1}{bh}(x-b)(t-h) \ , \quad -\frac{1}{bh} x (t-h) \ , \quad -\frac{1}{bh}(x-b) t \ , \quad \frac{1}{bh} x \, t \right] \ . \tag{14}$$

Displacements are computed from velocities by integration

$$u(x,t) = u(x,0) + \int_0^t (N_1 v_1 + \ldots + N_4 v_4)\,\mathrm{d}t = u(x,0) + \int_0^t \mathbf{N}^*\,\mathbf{v}\,\mathrm{d}t\ . \tag{15}$$

Finally we have

$$u(x,t) = u(x,0) + \frac{xt^2}{2bh}(v_1 - v_2 - v_3 + v_4) + \frac{x}{b}(-v_1 + v_2) + \frac{t^2}{2h}(-v_1 + v_3) + v_1 t\ \ . \tag{16}$$

Derivative $\partial u/\partial x$ can also be computed

$$\partial u/\partial x = \frac{t^2}{2bh}(v_1 - v_2 - v_3 + v_4) + \frac{t}{b}(-v_1 + v_2) + \frac{\mathrm{d}u}{\mathrm{d}t}|_{t=0}\ . \tag{17}$$

The proper choice of virtual functions v^* is a fundamental question of the space-time approach. Different functions result in solution schemes of different properties: accuracy and stability. We propose a simple form with distribution δ in $t = \alpha h$

$$v^*(x,t) = \delta(t - \alpha h)\left[(1 - \frac{x}{b})v_3 + \frac{x}{b}\,v_4\right]\ . \tag{18}$$

Required derivatives of virtual v^* and real v functions can be determined from (18) and (13)

$$\frac{\partial v^*}{\partial x} = \frac{1}{b}(-v_3 + v_4)\ , \tag{19}$$

$$\frac{\partial v}{\partial t} = \frac{x}{bh}(v_1 - v_2 - v_3 + v_4) + \frac{1}{h}(-v_1 + v_3)\ . \tag{20}$$

We notice that the Dirac δ term in the subintegral function reduces the integration in Ω to the integration over $0 \le x \le b$. Finally the Eqn. (12) can be written in the following matrix form:

$$\begin{aligned}
&\rho A \int_0^b \begin{bmatrix} -\left(\frac{x}{b} - 1\right) \\ \frac{x}{b} \end{bmatrix} \left[\frac{x}{bh} - \frac{1}{h},\ -\frac{x}{bh},\ -\frac{x}{bh} + \frac{1}{h},\ \frac{x}{bh}\right] \mathrm{d}x + \\
&+ N \int_0^b \begin{bmatrix} -\frac{1}{b} \\ \frac{1}{b} \end{bmatrix} \left[\frac{t^2}{2bh} - \frac{t}{b},\ -\frac{t^2}{2bh} + \frac{t}{b},\ -\frac{t^2}{2bh},\ \frac{t^2}{2bh}\right] \mathrm{d}x\Big|_{t=\alpha h} - \\
&- \eta \int_0^b \begin{bmatrix} -(\frac{x}{b} - 1) \\ \frac{x}{b} \end{bmatrix} \left[\frac{(x-b)(t-h)}{bh},\ -\frac{x(t-h)}{bh},\ -\frac{(x-b)t}{bh},\ \frac{xt}{bh}\right] \mathrm{d}x\Big|_{t=\alpha h} = 0\ .
\end{aligned} \tag{21}$$

The resulting matrices are listed below:

$$\mathbf{M} \ = \ \frac{\rho b}{h} \left[\begin{array}{cc|cc} -\frac{1}{3} & -\frac{1}{6} & \frac{1}{3} & \frac{1}{6} \\ -\frac{1}{6} & -\frac{1}{3} & \frac{1}{6} & \frac{1}{3} \end{array}\right] = \frac{1}{h}\left[-\mathbf{M}_s \mid \mathbf{M}_s\right] \tag{22}$$

$$\begin{aligned}
\mathbf{K} \ &= \ \frac{Nh}{b} \left[\begin{array}{cc|cc} \alpha(1-\frac{\alpha}{2}) & -\alpha(1-\frac{\alpha}{2}) & \frac{\alpha^2}{2} & -\frac{\alpha^2}{2} \\ -\alpha(1-\frac{\alpha}{2}) & \alpha(1-\frac{\alpha}{2}) & -\frac{\alpha^2}{2} & \frac{\alpha^2}{2} \end{array}\right] = \\
&= h\left[\alpha(1 - \frac{\alpha}{2})\mathbf{K}_s \mid \frac{\alpha^2}{2}\mathbf{K}_s\right]
\end{aligned} \tag{23}$$

$$\mathbf{C} \ = \ \eta b \left[\begin{array}{cc|cc} \frac{1-\alpha}{3} & \frac{1-\alpha}{6} & \frac{\alpha}{3} & \frac{\alpha}{6} \\ \frac{1-\alpha}{6} & \frac{1-\alpha}{3} & \frac{\alpha}{6} & \frac{\alpha}{3} \end{array}\right] = \left[(1-\alpha)\mathbf{C}_s \mid \alpha\mathbf{C}_s\right] \tag{24}$$

$\mathbf{M}$, $\mathbf{K}$, and $\mathbf{C}$ are the space-time inertia, stiffness and viscous damping matrices, respectively. We notice that they are composed of two square matrices, each of a dimension equal to the number of degrees of freedom in a spatial finite element. Matrices $\mathbf{M}_s$, $\mathbf{K}_s$, and $\mathbf{C}_s$ have the same or similar form to respective matrices derived traditionally from the classical finite element approach. The final form of the motion equation establishes the force equilibrium on the edge of the element domain Ω. Vector $\mathbf{v}$ contains nodal velocities $\mathbf{v}_i$ at the initial time $t = t_i$ and $\mathbf{v}_{i+1}$ at the final time $t = t_i + h$.

$$(\mathbf{M} + \mathbf{C} + \mathbf{K}) \left\{ \begin{array}{c} \mathbf{v}_i \\ \mathbf{v}_{i+1} \end{array} \right\} + \mathbf{e} = \mathbf{0} \quad \text{or} \quad \mathbf{K}^* \, \mathbf{v} + \mathbf{e} = \mathbf{0} \ . \tag{25}$$

The velocity vector $\mathbf{v}_{i+1}$ is the only unknown vector in the above step-by-step equation. Finally we must compute displacements $\mathbf{q}_{i+1}$. We use the formula

$$\mathbf{q}_{i+1} = \mathbf{q}_i + h[\beta \, \mathbf{v}_i + (1 - \beta) \, \mathbf{v}_{i+1}] \tag{26}$$

The stability analysis results in $\beta = 1 - \alpha$.

4.2 Discretization of the string element carrying moving mass

The last term $\delta(x - v_m t) \, m \, \partial^2 u(v_m t, t)/\partial t^2$ in the motion equation (1) describes the inertial moving mass. $\partial^2 u(v_m t, t)/\partial t^2$ is the vertical acceleration of the moving mass and at the same time the acceleration of the point of the string in which the mass is temporarily placed (it is $x = x_0 + v_m t$). The acceleration of the mass $\partial^2 u(v_m t, t)/\partial t^2$ moving with a constant velocity v_m, according to the Renaudot formula (which in fact is the chain rule of differentiation), results in three terms:

$$\frac{\partial^2 u(v_m t, t)}{\partial t^2} \ = \ \frac{\partial^2 u(x,t)}{\partial t^2}\bigg|_{x=v_m t} + \ 2 v_m \, \frac{\partial^2 u(x,t)}{\partial x \partial t}\bigg|_{x=v_m t} + \ v_m^2 \, \frac{\partial^2 u(x,t)}{\partial x^2}\bigg|_{x=v_m t} . \tag{27}$$

Thus we can separate the transverse acceleration, the Coriolis acceleration, and the centrifugal acceleration, respectively. This is the so-called Renaudot notation for the constant speed v_m. Another one, the so-called Jakushev notation (or approach) finally gives the same result in our case of the constant mass m.

In our space-time finite element method we formulate equations in terms of velocities. The mass acceleration $\frac{\partial^2 u(v_m t, t)}{\partial t^2}$ is expressed in terms of velocities aswell:

$$\frac{\partial^2 u(v_m t, t)}{\partial t^2} \ = \ \frac{\partial v(v_m t, t)}{\partial t} \ = \ \frac{\partial v(x,t)}{\partial t}\bigg|_{x=v_m t} + \ v_m \, \frac{\partial v(x,t)}{\partial x}\bigg|_{x=v_m t} . \tag{28}$$

The first term on the right-hand side states the real inertia (when multiplied by m) and the second term (also multiplied by m) expresses forces similar to damping forces.

In the final stage three resulting matrices are responsible for transverse inertia (the matrix has the form of the inertia matrix), damping forces (the matrix multiplied by the velocity vector has a form similar to the Coriolis forces) and stiffness (potential) forces (the matrix, if multiplied by the velocity vector, has a form similar to the centrifugal forces). The third matrix appears as the result of initial displacements in the time interval.

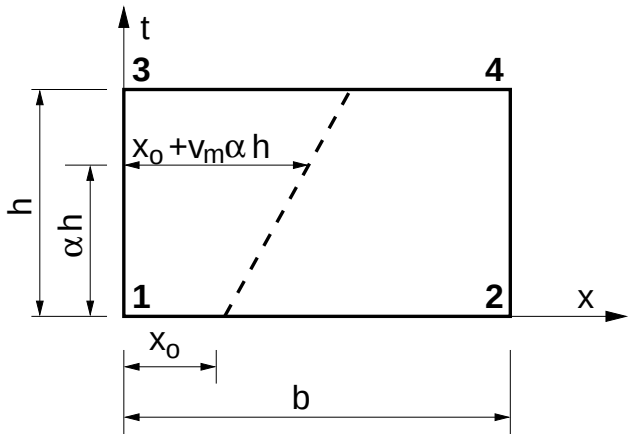

Figure 6: Mass path in the space-time finite element.

Let us now follow this idea and treat numerically the right-hand side inertial term of (1). The same mathematical steps as in the case of pure string enables us to integrate the inertial term

$$\int_0^h \int_0^b \mathbf{N}^* m\delta(x - v_m t) \frac{\partial^2 u(x_0 + v_m t, t)}{\partial t^2} \, \mathrm{d}x, \mathrm{d}t \ . \tag{29}$$

We consider first the integral term of (15). We use the same linear interpolation of the velocity (13). The virtual velocity v^*:

$$v^*(x,t) = \mathbf{N}^* \, \dot{\mathbf{q}}_p = \delta(t - \alpha h) \begin{bmatrix} 1 - \frac{x}{b} \\ \frac{x}{b} \end{bmatrix} \dot{\mathbf{q}}_p \tag{30}$$

Consequent integration results in two matrices: the moving mass inertia matrix $\mathbf{K}_m$

$$\mathbf{M}_m \ = \ \frac{m}{h} \left[\begin{array}{cc|cc} -(1-\kappa)^2 & -\kappa(1-\kappa) & (1-\kappa)^2 & \kappa(1-\kappa) \\ -\kappa(1-\kappa) & -\kappa^2 & \kappa(1-\kappa) & \kappa^2 \end{array} \right] \ , \tag{31}$$

where $\kappa = (x_0 + v_m \alpha h)/b$, x_0 is a starting position of the mass in the space-time element (at $t = t_0$) (see Fig. 6), and the moving mass damping matrix $\mathbf{C}_m$

$$\mathbf{C}_m = \frac{m v_m}{b} \left[\begin{array}{cc|cc} -(1-\kappa)(1-\beta) & (1-\kappa)(1-\beta) & -(1-\kappa)\beta & (1-\kappa)\beta \\ -\kappa(1-\beta) & \kappa(1-\beta) & -\kappa\beta & \kappa\beta \end{array} \right] \ . \tag{32}$$

Let us now consider the contribution of $u(x,0)$ in (15). We integrate by parts the virtual work

$$v_m^2 \int_0^h \int_0^b v^* \frac{\partial^2 u_0}{\partial x^2} \mathrm{d}x\mathrm{d}t = -v_m^2 \int_0^h \int_0^b \frac{\partial v^*}{\partial x} \frac{\partial u_0}{\partial x} \mathrm{d}x\mathrm{d}t \tag{33}$$

Since displacements of the left and right node of the element are expressed by $u_L = u_L^0 + h[\beta v_1 + (1-\beta)v_3]$ and $u_R = u_R^0 + h[\beta v_2 + (1-\beta)v_4]$, we can derive the required $\mathrm{d}u_0/\mathrm{d}x$

$$\frac{\mathrm{d}u_0}{\mathrm{d}x} = \frac{u_R - u_L}{b} = \frac{u_R^0 - u_L^0}{b} + \frac{h}{b}[-\beta v_1 + \beta v_2 - (1-\beta)v_3 + (1-\beta)v_4] \tag{34}$$

Numbering of nodes is presented in Fig. 6. Matrix $\mathbf{K}_m$ is the stiffness mass matrix

$$\mathbf{K}_m = \frac{h m v_m^2}{b^2} \left[\begin{array}{cc|cc} \beta & -\beta & 1-\beta & -(1-\beta) \\ -\beta & \beta & -(1-\beta) & 1-\beta \end{array} \right] \tag{35}$$

The term $(u_R^0 - u_L^0)/b$ in (34) multiplied by mv_m^2/b results in initial nodal forces $\mathbf{e}$ in the space-time layer (25).

5 Numerical results

The numerical results obtained with the proposed space-time approach can be compared with the analytical solution. Moreover, the spring-mass finite element solution can also be plotted. In our tests the string was discretized by a set of 200 finite elements. The time step h was equal to $b/40v_m$. It means, that the mass passes from joint to joint in 40 time steps. We assume m=1.0, ρA=1.0, l=1.0, N=1. Results obtained by the space-time finite element method are presented in Fig. 7. We notice that at lower speed, up to 0.3-0.4c the coincidence with semi-analytical results is almost perfect. We observe the convergence of results to the semi-analytical solution with decreasing time step and increasing number of spatial elements. Unfortunately, the convergency rate is low. At higher speed the total time of simulation is shorter and lower number of time steps is required to reach the end support during the mass motion. All important features of resulting curves, especially high gradients of displacements near the end support are represented then with lower accuracy. The error analysis of the method allows us to say that in a general case the error is equal to $h^2(1/2 - \alpha) + \mathcal{O}h^3$. In the particular case $\alpha = 0.5$ the error equals to $1/12h^3 + \mathcal{O}h^4$. However, in this case the time integration sheme of the space-time finite element method is conditionally stable. The gap between numerical and semi-analytical results is visible in both diagrams. The plot for $\alpha = 1/2$ is visually better at higher speed range.

Higher velocity can also be considered. Fig. 8 presents displacements in time of the particle for $0.9 \leq v_m/c \leq 1.2$. We notice a good coincidence of the plot with the expected zero line. Further examples prove the efficiency and accuracy of the approach. One can plot the displacements of selected fixed points of the string. In such a case results exhibit very good coincidence with the analytical-numerical approach.

We can compare our results with displacements of the contact point of the string under the travelling oscillator (Fig. 9). We notice the significant difference, especially for higher speed range, between semi-analytical results or space-time finite element approach and curves obtained for the oscillator. Pure mass can not be replaced in computations by the oscillator for problems of high moving mass influence, ie. for the velocity higher then 0.3-0.5 of the wave speed and for moving mass to the string mass ratio higher then 0.2.

6 Conclusions

In this paper we dealt with numerical analysis of string vibrations under the moving inertial load. We derived the matrix formula of the time integration procedure on the base of the space-time finite element method. Solutions presented in the literature are derived from the base of classical time integration schemes. Published results are acceptable for low speed of the travelling mass. In such a case errors in formulations do not contribute visible difference in results. In common practise massless force acting on the string in the form of oscillator is applied. Such results are greatly underestimated, and for the velocity higher than 0.2–0.3c they cannot be taken into account.

The approach presented in this paper can be applied for the whole range of the speed, up to the wave speed $v_m = c$. The precision of results is high. In the case of the speed higher than the wave speed the particle's trajectory is close to the theoretical zero line. Discontinuities

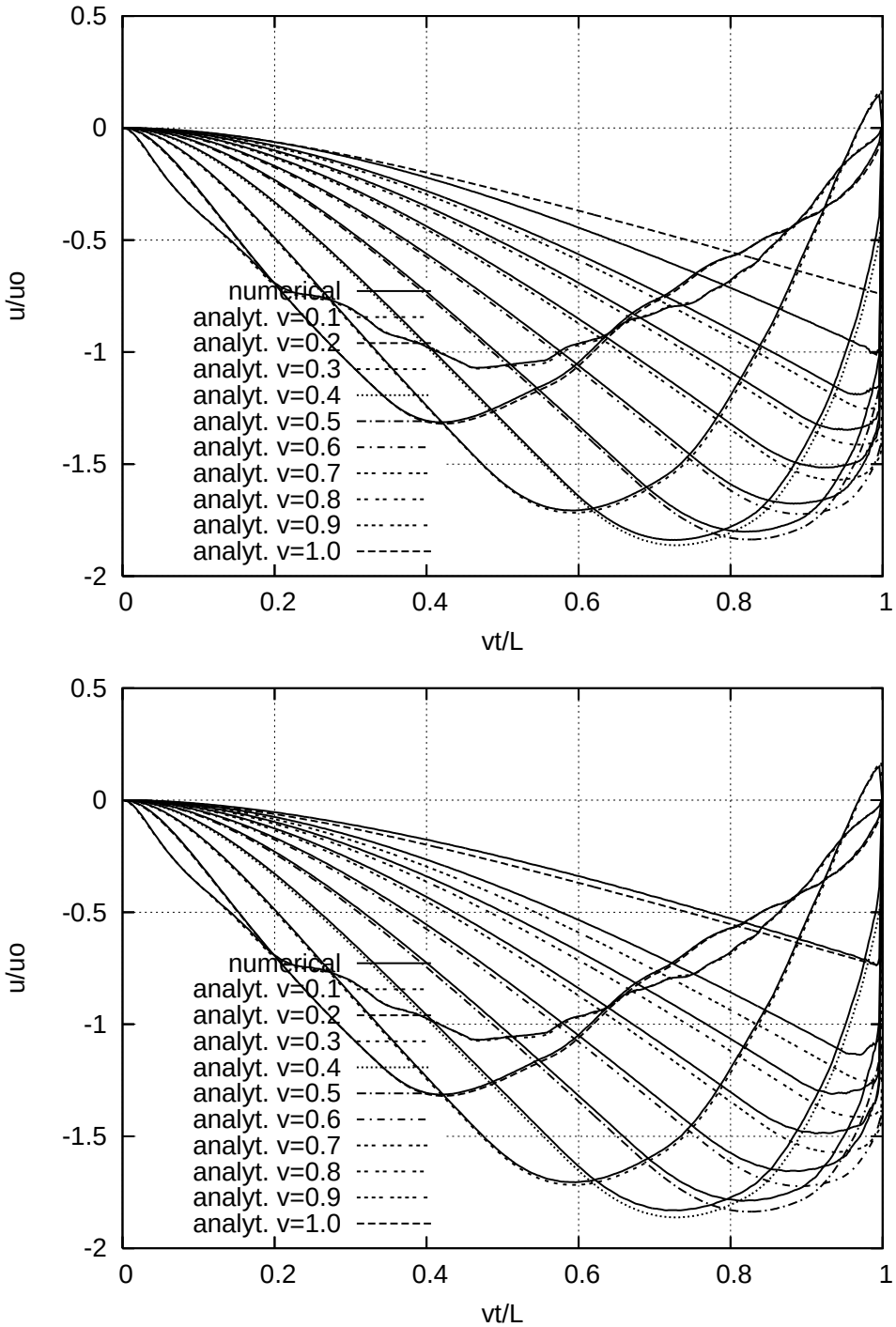

Figure 7: Displacements under moving mass – space-time finite element solution for $\alpha = 0.5$ (upper) and $\alpha = 1.0$ (lower) compared with semi-analytical solution.

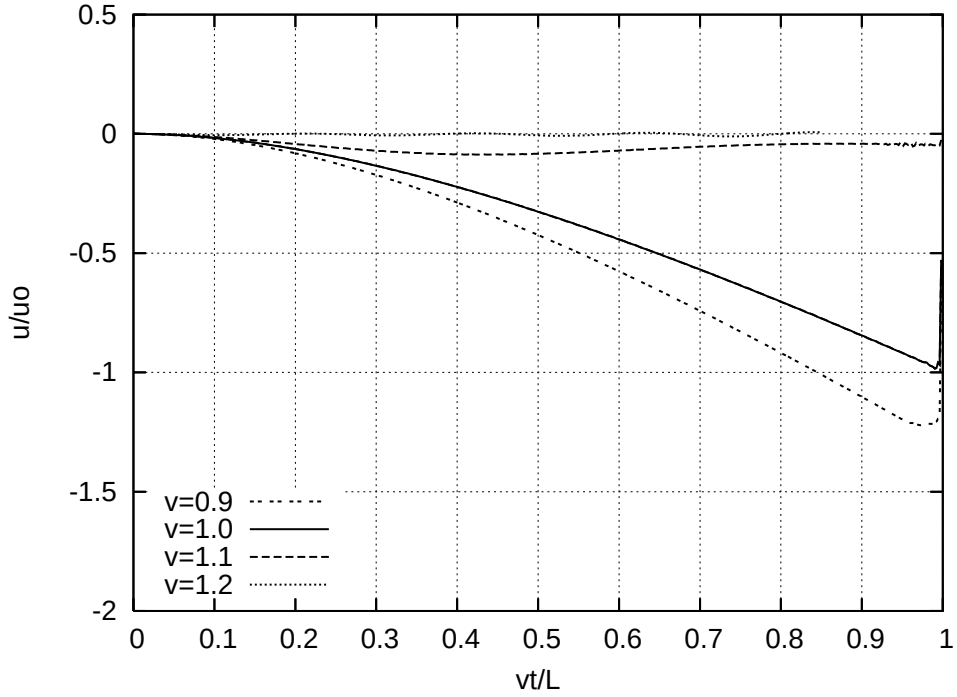

Figure 8: Displacements under moving mass for v_m equal to 0.9, 1.0, 1.1 and 1.2 c.

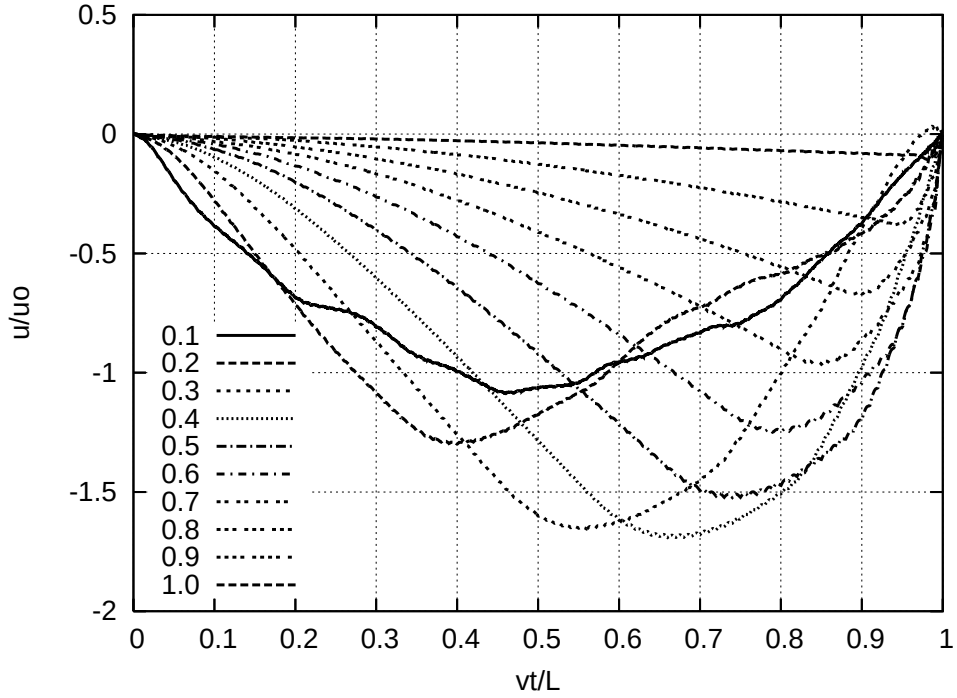

Figure 9: Finite element solution – displacements of the string under the oscillator for the speed v=0.1—1.0.

at $x = l$ exhibited and proven analytically are easily visible in figures presenting numerical trajectories.

The method presented in this paper can be successfully applied to other structures subjected by inertial load: beams, frames, and plates. Moreover, the space-time finite element approach can be adapted to classical time integration schemes (Newmark, etc.).

References

[1] Bajer C, Bohatier C. The soft way method and the velocity formulation. *Comput. and Struct.* 1995; **55**(6):1015–1025.

[2] Stokes G. Discussion of a differential equation relating to the breaking railway bridges. *Trans. Cambridge Philosoph. Soc.* 1849; **Part 5**:707–735. Reprinted in: Mathematical and Physical Papers, Cambridge, Vol.II, 1883, pp.179-220.

[3] Frỳba L. *Vibrations of solids and structures under moving loads*. Academia: Prague, 1972.

[4] Saller H. *Einfluss bewegter Last auf Eisenbahnoberbau und Brücken*. Berlin und Wiesbaden, 1921.

[5] Inglis C. *A Mathematical Treatise on Vibrations in Railway Bridges*. Cambridge University Press, 1934.

[6] Schallenkamp A. Schwingungen von Trägern bei bewegten Lasten. *Arch. of Appl. Mech. (Ingenieur Archiv)* June 1937; **8**(3):182–198.

[7] Smith C. Motion of a stretched string carrying a moving mass particle. *J. Appl. Mech.* 1964; **31**(1):29–37.

[8] Szcześniak W. Inertial moving loads on beams (in Polish). Scientific Reports, Technical University of Warsaw, Civil Engineering 112 1990.

[9] Wu JJ. Dynamic analysis of an inclined beam due to moving loads. *J. Sound and Vibr.* 2005; **288**:107–131.

[10] Metrikine A, Verichev S. Instability of vibration of a moving oscillator on a flexibly supported Timoshenko beam. *Archive of Applied Mechanics* 2001; **71**(9):613–624.

[11] Pesterev A, Bergman L, Tan C, Tsao TC, Yang B. On asymptotics of the solution of the moving oscillator problem. *J. Sound and Vibr.* 2003; **260**:519–536.

[12] Biondi B, Muscolino G. New improved series expansion for solving the moving oscillator problem. *J. Sound and Vibr.* 2005; **281**:99–117.

[13] Andrianov I, Awrejcewicz J. Dynamics of a string moving with time-varying speed. *J. Sound and Vibr.* 2006; **292**:935–940.

[14] Michaltsos GT. Dynamic behaviour of a single-span beam subjected to loads moving with variable speeds. *J. Sound and Vibr.* 2002; **258**(2):359–372.

[15] Gavrilov S, Indeitsev D. The evolution of a trapped mode of oscillations in a string on an elastic foundation — moving inertial inclusion system. *J. Appl. Math. and Mech.* 2002; **66**(5):852–833.

[16] Gavrilov S. The effective mass of a point mass moving along a string on a Winkler foundation. *J. Appl. Math. and Mech.* 2006; **70**(4):641–649.

[17] Rodeman R, Longcope D, Shampine L. Response of a string to an accelerating mass. *J. Appl. Mech.* 1976; **98**(4):675–680.

[18] Kaplunov Y. The torsional oscillations of a rod on a deformable foundation under the action of a moving inertial load (in Russian). *Izv. Akad. Nauk SSSR, MTT* 1986; **6**:174–177.

[19] Filho F. Finite element analysis of structures under moving loads. *The Shock and Vibration Digest* 1978; **10**(8):27–35.

[20] Rieker J, Lin YH, Trethewey M. Discretization considerations in moving load finite element beam models. *Finite Elements in Analysis and Design* 1996; **21**:129–144.

[21] Rieker J, Trethewey M. Finite element analysis of an elastic beam structure subjected to a moving distributed mass train. *Mechanical Systems and Signal Processing* 1999; **13**(1):31–51.

[22] Bajer C. Triangular and tetrahedral space–time finite elements in vibration analysis. *Int. J. Numer. Meth. Engng.* 1986; **23**:2031–2048.

[23] Bajer C. Notes on the stability of non–rectangular space–time finite elements. *Int. J. Numer. Meth. Engng.* 1987; **24**:1721–1739.

[24] Bajer C. Adaptive mesh in dynamic problem by the space–time approach. *Comput. and Struct.* 1989; **33**(2):319–325.

[25] Bajer C, Bogacz R, Bonthoux C. Adaptive space–time elements in the dynamic elastic–viscoplastic problem. *Comput. and Struct.* 1991; **39**:415–423.

[26] Bajer C, Bonthoux C. State–of–the–art in the space–time element method. *Shock Vibr. Dig.* 1991; **23**(5):3–9.

[27] Bajer C. Space–time finite element formulation for the dynamical evolutionary process. *Appl. Math. and Comp. Sci.* 1993; **3**(2):251–268.

[28] Gurtin M. Variational principles for linear elastodynamics. *Arch. Rat. Mech. Anal.* 1964; **16**:34–50.

[29] Oden J. A generalized theory of finite elements, II. Applications. *Int. J. Numer. Meth. Engng.* 1969; **1**:247–259.

[30] Fried I. Finite element analysis of time–dependent phenomena. *AIAA J.* 1989; **7**:1170–1173.

[31] Argyris J, Scharpf D. Finite elements in time and space. *Aeron. J. Roy. Aeron. Soc.* 1969; **73**:1041–1044.

[32] Argyris J, Scharpf D. Finite elements in space and time. *Nucl. Engng Design* 1969; **10**:456–469.

[33] Kuang Z, Atluri S. Temperature field due to a moving heat source. *J. Appl. Mech. Trans. ASME* 1985; **52**:274–280.

[34] Kączkowski Z. The method of finite space–time elements in dynamics of structures. *J. Tech. Phys.* 1975; **16**(1):69–84.

[35] Kączkowski Z. General formulation of the stiffness matrix for the space–time finite elements. *Archiwum Inż. Ląd.* 1979; **25**(3):351–357.

[36] Kączkowski Z, Langer J. Synthesis of the space–time finite element method. *Archiwum Inż. Ląd.* 1980; **26**(1):11–17.

[37] Bajer C. Dynamics of contact problem by the adaptive simplex–shaped space–time approximation. *J. Theor. Appl. Mech.* 1988; **7**:235–248. Special issue, suplement No. 1.

[38] Bajer C. The space-time approach to rail/wheel contact and corrugations problem. *Comp. Ass. Mech. Eng. Sci.* 1998; **5**(2):267–283.

[39] Bohatier C. A large deformation formulation and solution with space–time finite elements. *Arch. Mech.* 1992; **44**:31–41.

[40] Dyniewicz B, Bajer C. Inertial load moving on a string – discontinuous solution. *Theoretical Foundations in Civil Engineering*, Szcześniak W (ed.), OWPW Warsaw, 2007; 141–150.